Supplemental Data: An Agent-Based Systems Pharmacology Model of the Antibody Drug Conjugate Kadcyla to Predict Efficacy of Different Dosing Regimens

Bruna Menezes[*], Cornelius Cilliers[*], Timothy Wessler[*], Greg M. Thurber[*#], and Jennifer Linderman[*#]

[*] Department of Chemical Engineering, University of Michigan, Ann Arbor, MI 48109

[#] Department of Biomedical Engineering, University of Michigan, Ann Arbor, MI 48109

Supplementary Data

Supplemental Figures

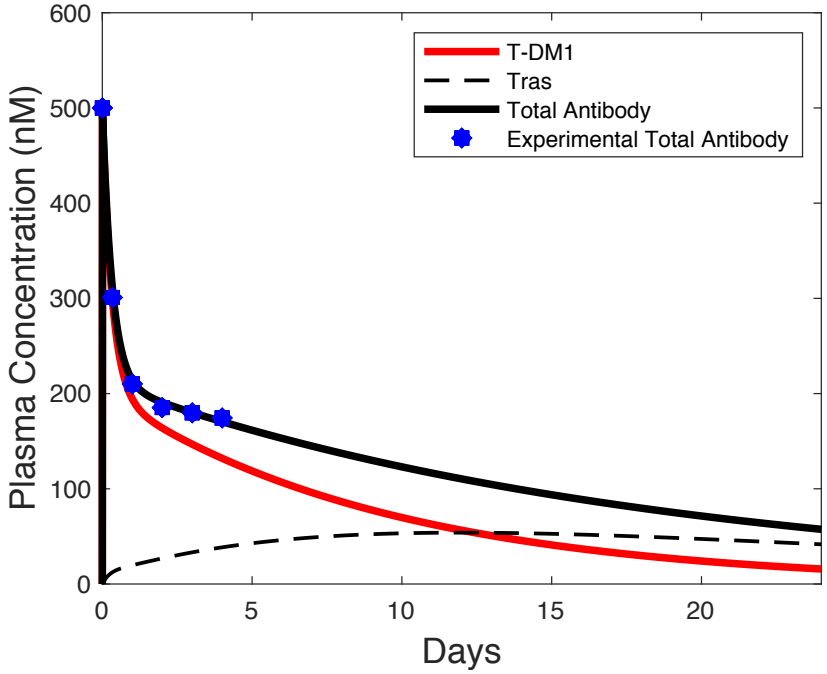

Figure S1: T-DM1 plasma clearance. Rates for antibody and T-DM1 clearance (CL_{TT}, CL_2, CL_{DEC}) were calibrated to experimental data (1) and literature (2).

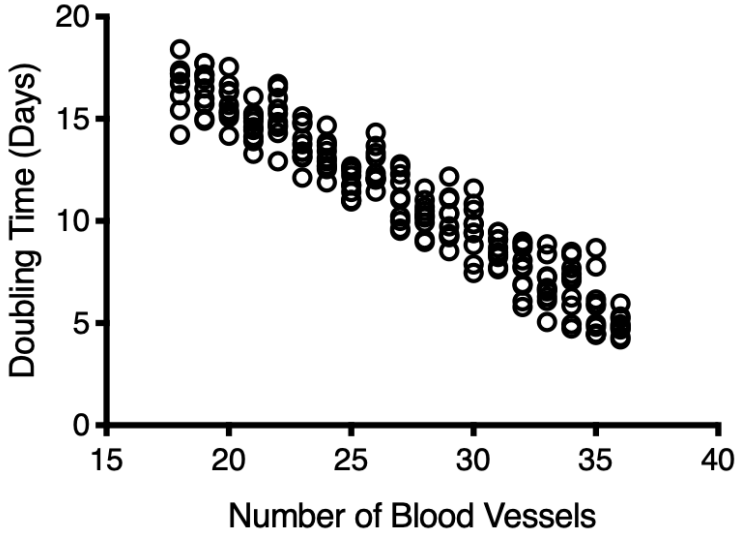

Figure S2: Relationship between blood vessel density and doubling time. Tumors with lower blood vessel density should have a higher cell doubling time t_d to account for hypoxic areas which often show lower proliferation (3). Here, we assume a linear relationship between the ranges of possible number of vessels for the simulation (18 - 36) and the doubling time (5 - 17 days). For each simulation, the doubling time is chosen from a normal distribution in which the mean is provided from this linear relationship, and the standard deviation is 1 day. Ten simulations with each value of blood vessel density are plotted to demonstrate the corresponding doubling time.

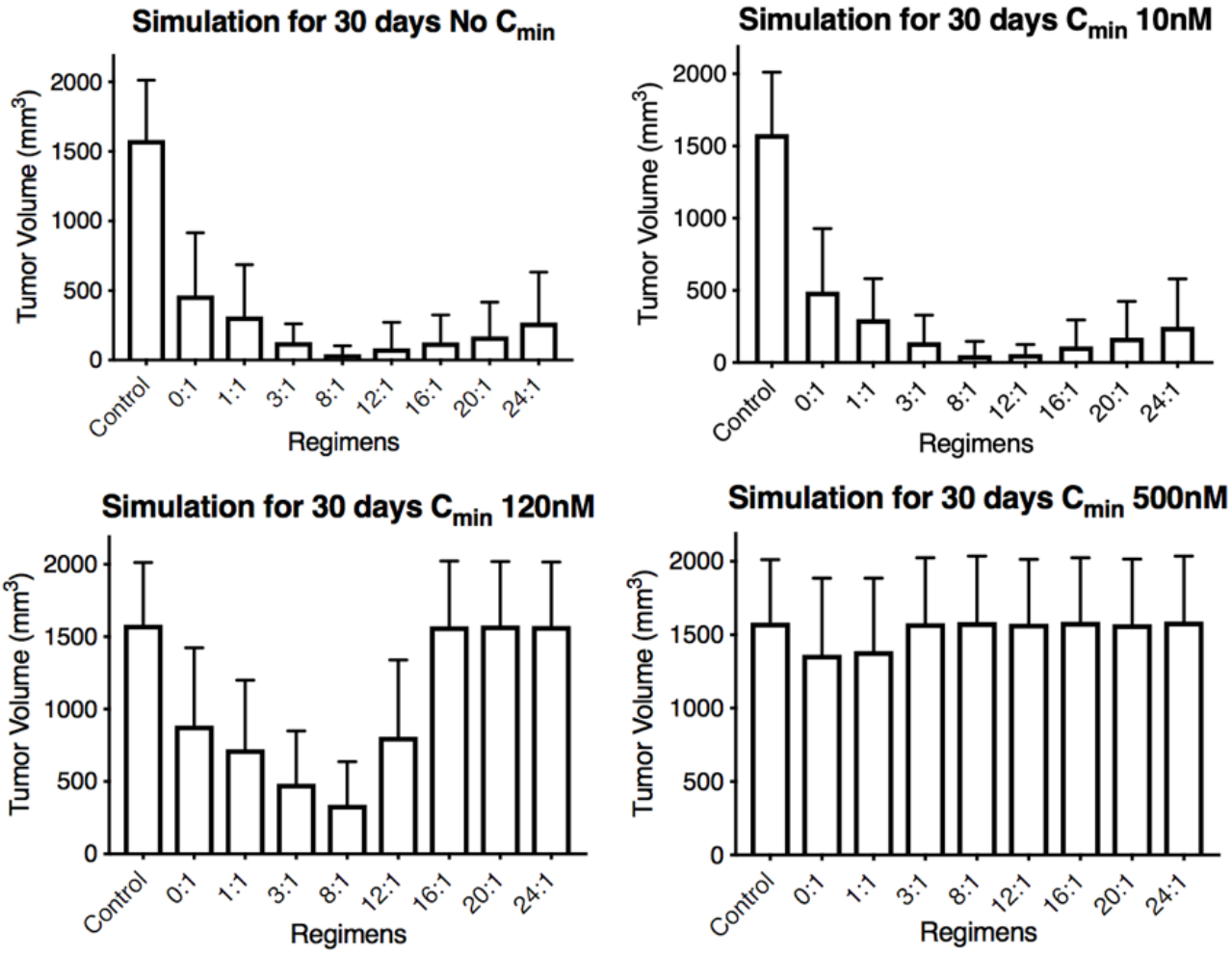

Figure S3: Comparison of treatment regimen for drugs with different C_{min}. Prediction of regimens with coadministration of trastuzumab and T-DM1 with a hypothetical without minimum threshold and for 10nM, 120nM, and 500nM C_{min} at 30 days.

A.

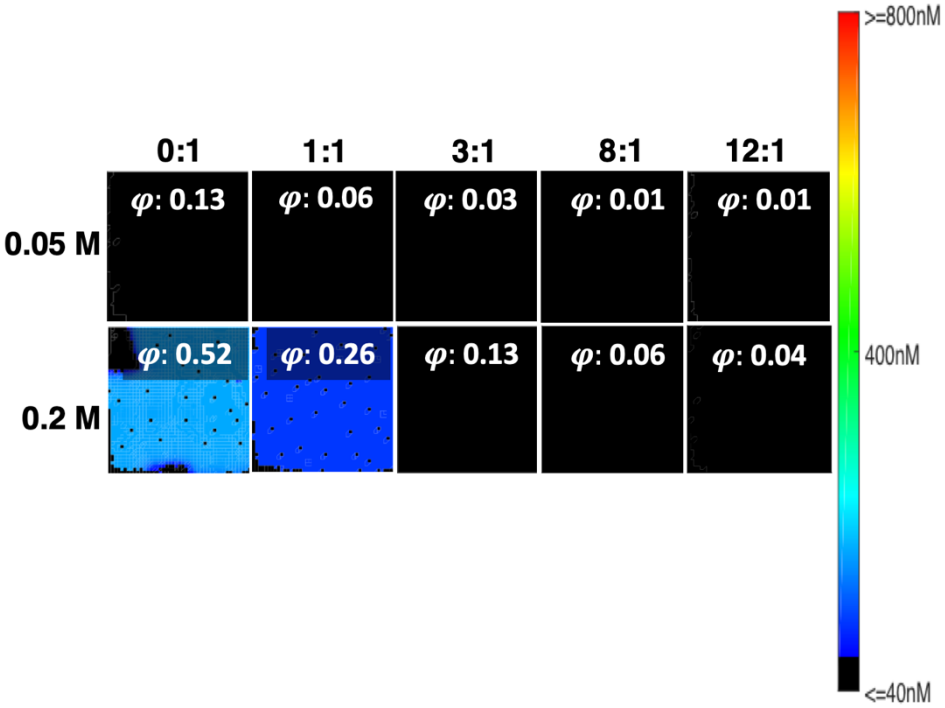

B.

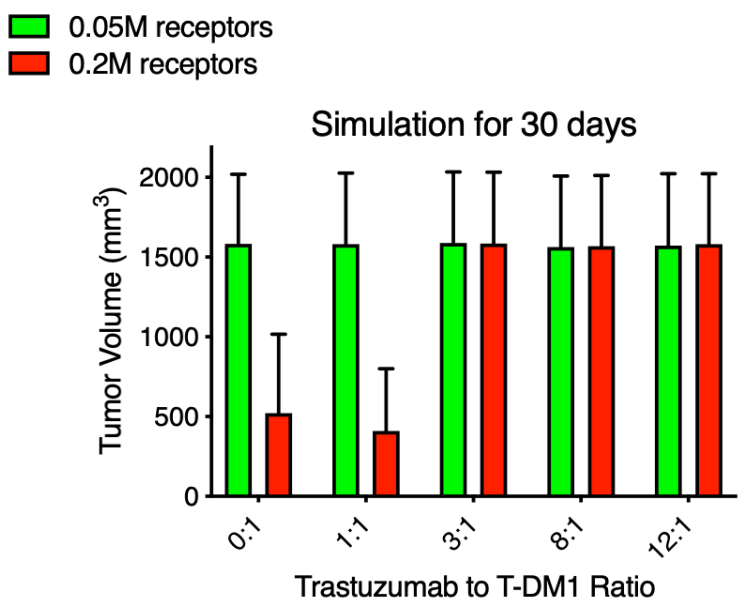

Figure S4: Distribution and efficacy for tumors with an average of 50,000 receptors/cell and comparison with 0.2M. A. T-DM1 bound for 0:1, 1:1, 3:1, 8:1, and 12:1 distribution and comparison with distribution 200,000 receptors/cell with Thiele modulus displayed. B. Efficacy predictions for 50,000 and 200,000 receptor/cell tumors at 30 days. There is no efficacy for tumors with 50,000 receptors/cell even at clinical doses.

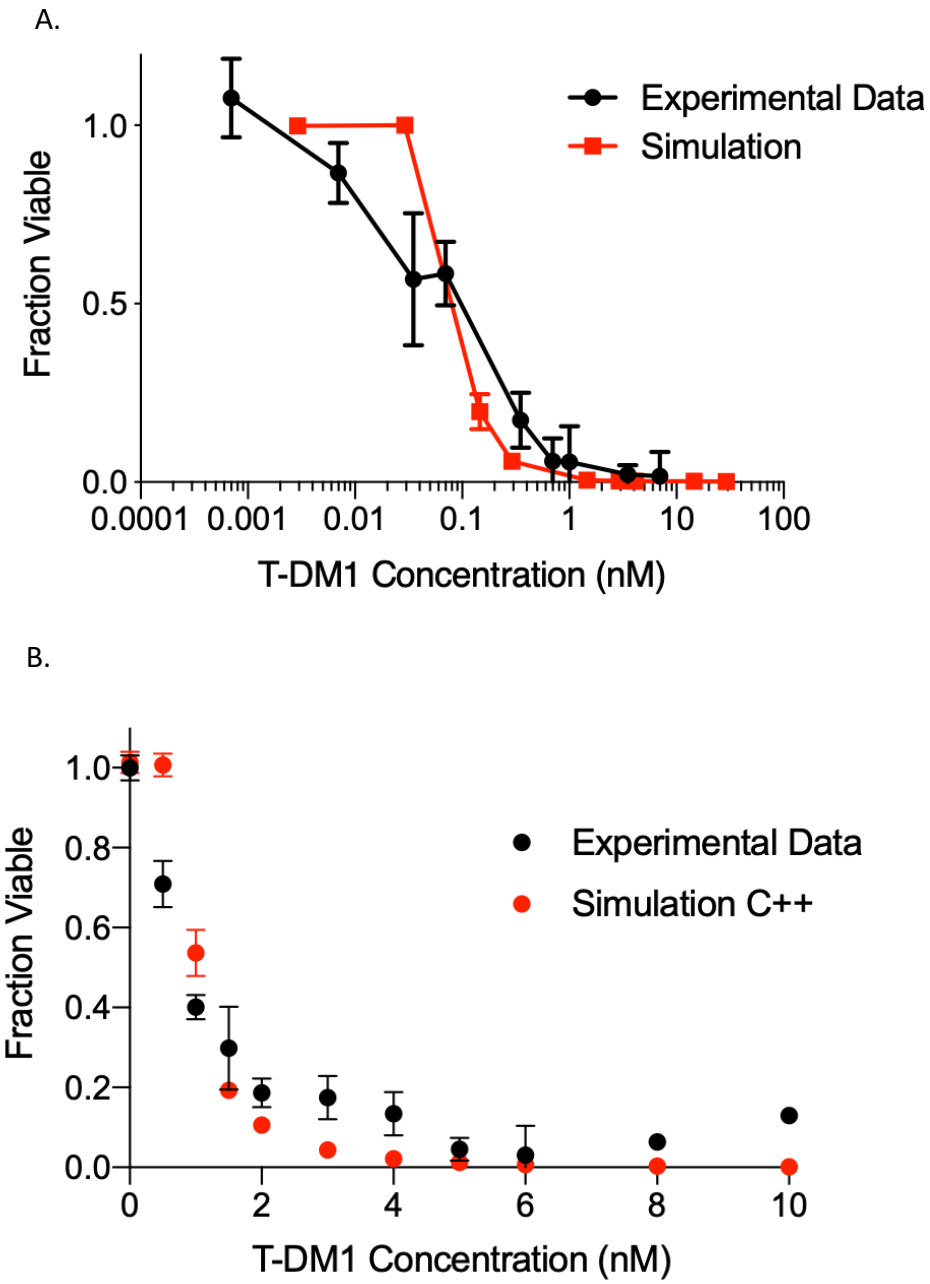

Figure S5: *In vitro s*imulations and comparison with experimental data(4). A. Toxicity assay showing the fraction of viable NCI-N87 cells incubated for 6 days with different concentrations of ado-trastuzumab emtansine (T-DM1). B. Viability of NCI-N87 cells following coincubation of trastuzumab and T-DM1 ratio (kept at a constant total antibody concentration of 10 nM and varying the fraction of T-DM1) and comparison with experimental data (normalized to trastuzumab treatment account for the effect of trastuzumab alone). Both of these results indicate that the cell killing parameters fit to the *in vivo* data are similar to the sensitivity *in vitro*.

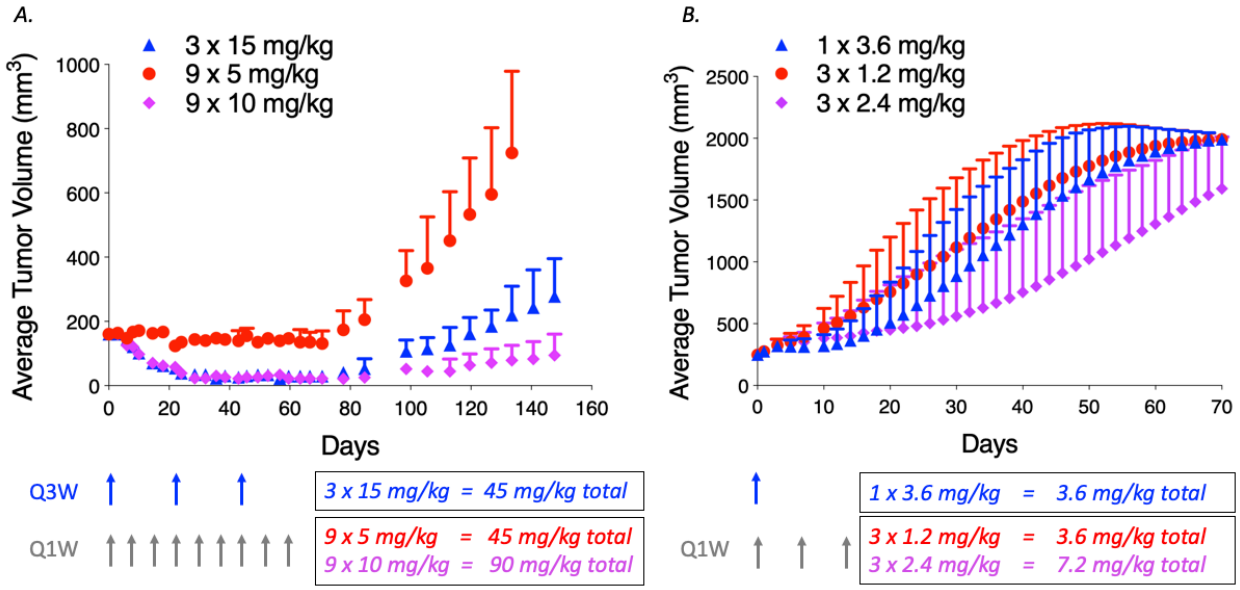

Figure S6: Fractionation of T-DM1 and qualitative comparison with literature. A) Results from Jumbe, N. et al. using a BT474EEI xenograft model that is resistant to trastuzumab (5). Data was extracted using 'Data Thief' software. Fractionated dosing leads to worse overall efficacy, but with higher total doses (enabled by fractionated dosing), the efficacy improves. B) The model simulation for fractionated dosing in NCI-N87 cells is replotted from the manuscript for convenience. The dose frequency (once weekly 'Q1W' versus every three weeks 'Q3W') and dose escalation enabled by fractionation (2-fold increase) are the same for both studies, but the doses and number of cycles are different. Note that the x and y axes are also different. Despite these differences, the overall trend is the same: fractionation has similar or worse efficacy compared to single dosing, but fractionated dosing can improve efficacy if it enables larger total doses to be administered.

Supplemental Methods

1. Vessel Density Determination

To determine the number of vessels to include in simulations, we analyzed images of mouse tumor slices that were stained *ex-vivo* with CD31-AF555 to show blood vessels. Images were processed in MATLAB to find the vessel density (4). Briefly, random lines are placed on the images, and the number of cuts is counted. Based on that, we can find the surface of the blood vessel over tumor volume ratio (S/V) from (6):

$$\frac{S}{V} = \frac{2c}{Ln}$$

where c is the number of cuts, L is the length of the line (μm), and n is the number of the lines placed. Here we used $75\mu m$ for L and 10000 lines. To match experimental data, we determined 18 to 36 blood vessels per initial simulation area (S/V range from 23/cm to 45/cm) is appropriate.

2. Cell Shuffling Algorithm

We assume that at all times cells are close to each other. After cell proliferation and removal of any dead cells from the grid, cells "shuffle" to fill empty grid compartments while also maintaining only one cell per grid compartment. First, cells shuffle to make room for all daughter cells that proliferated on that agent time step, and then the tumor contracts to remove all empty spaces inside the tumor.

For the tumor growth/expansion following cell division, two daughter cells are formed. One cell remains in the original grid compartment, and the other displaces the neighboring cell that is closest to an empty grid compartment or border. The newly displaced cell then displaces the next cell that is closest to that same empty grid compartment or border. If there is more than one empty grid compartment with the same distance, one of the compartments is chosen randomly. This shuffling algorithm repeats until only one cell occupies each grid space as shown below.

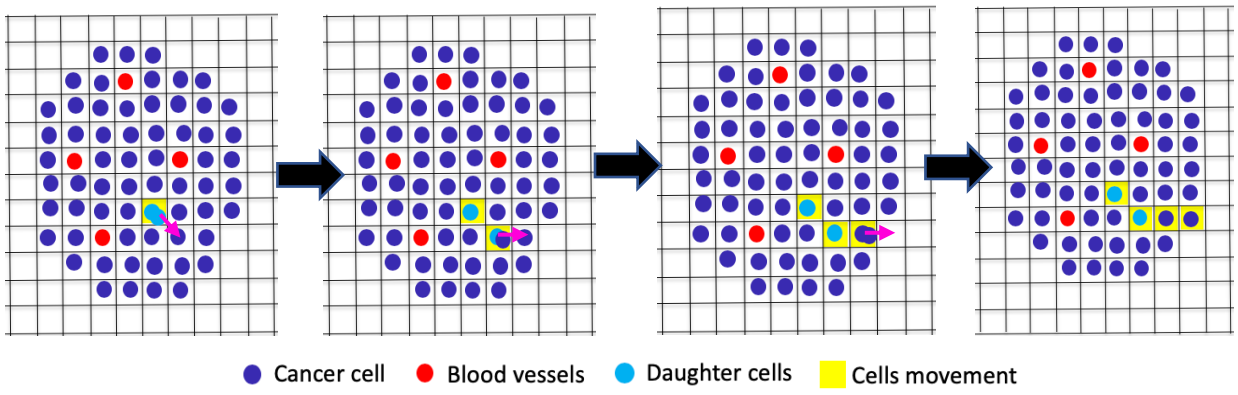

Figure S7: Shuffling of cells to make room for daughter cell on the grid.

Dead cells were estimated to leave the grid at 2.5 days based on observations of our published data, which show that maximum degradation occurs between 2 and 3 days and lower tumor volume decrease around 5 days (4). Model results have low sensitivity to this parameter (Figure S8). When a dead cell is removed from the grid, an empty grid compartment is left. In this

case, cells are shuffled from the farthest point on the border of the tumor (i.e. they collapse from the most protruding region of the tumor edge). This process is similar to the growth/expansion but in the opposite direction with the furthest cell displacing a neighboring cell that is closest to the empty grid compartment until a cell fills that empty grid compartment.

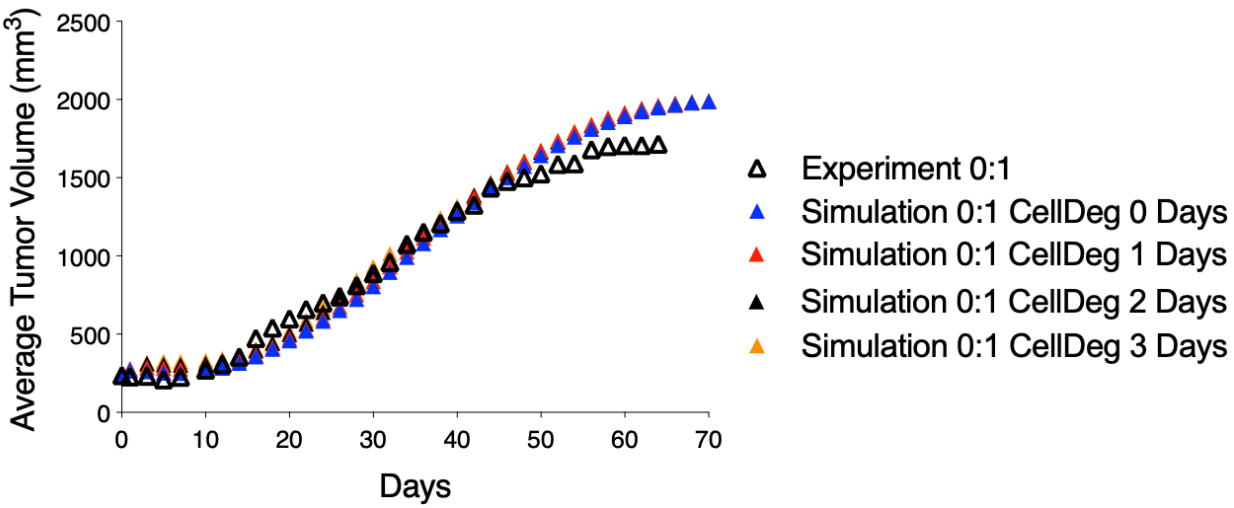

Figure S8: Effect of cell degradation time parameter on tumor volume. Simulations were run with cell degradation times varying from 0 - 3 days; the average of 100 simulations is plotted.

3. Estimating the minimum concentration of T-DM1 necessary to kill a cell

We estimated the minimum concentration of T-DM1 necessary to kill a cell, C_{min}, based on the concentration of T-DM1 *in vitro* that causes the first statistically significant drop in viability from *in vitro* data published in (4). We found that at least 5% of cell receptors on NCI-N87 cells (which have ~1 million receptors per cell) must be bound by T-DM1 for any efficacy. Assuming a steady state process, with internalization (k_e) and loss rate constants (k_{loss}) of 3.3 x 10^{-5} s^{-1} and 3.94 x 10^{-5} respectively:

$DM1_{in} * k_e = DM1_{out} * k_{loss}$ and $C_{min\ is}$ ~ 120nM.

The explicit inclusion of C_{min} in the pharmacodynamic model ensures that the simulations capture the scenario where the ADC is 'diluted' too much with unconjugated antibody, lowering efficacy. Otherwise, the model choice (e.g. using a Hill coefficient less than or equal to one) may eliminate this possibility. In such a scenario, the simulations would always predict maximum efficacy by adding enough antibody to saturate the tumor, regardless of the payload potency, receptor expression, internalization rate, etc. By adding C_{min} to these pharmacodynamic (PD) models, the results are less sensitive to the subjective choice of the PD model and therefore more robust.

References

1. Cilliers C, Nessler I, Christodolu N, Thurber GM. Tracking Antibody Distribution with Near-Infrared Fluorescent Dyes: Impact of Dye Structure and Degree of Labeling on Plasma Clearance. Mol Pharm. 2017;14(5):1623-33.
2. Bender B, Leipold DD, Xu K, Shen BQ, Tibbitts J, Friberg LE. A mechanistic pharmacokinetic model elucidating the disposition of trastuzumab emtansine (T-DM1), an antibody-drug conjugate (ADC) for treatment of metastatic breast cancer. AAPS J. 2014;16(5):994-1008.
3. Forster JC, Harriss-Phillips WM, Douglass MJ, Bezak E. A review of the development of tumor vasculature and its effects on the tumor microenvironment. Hypoxia (Auckl). 2017;5:21-32.
4. Cilliers C, Menezes B, Nessler I, Linderman J, Thurber GM. Improved tumor penetration and single-cell targeting of antibody–drug conjugates increases anticancer efficacy and host survival. Cancer Research. 2018;78(3):758-68.
5. Jumbe NL, Xin Y, Leipold DD, Crocker L, Dugger D, Mai E, et al. Modeling the efficacy of trastuzumab-DM1, an antibody drug conjugate, in mice. J Pharmacokinet Pharmacodyn. 2010;37(3):221-42.
6. Chalkley H, Cornfiel,J., Park, H. . A Method for Estimating Volume-Surface Ratios. Science. 1949;110:295-7.